

Article

Evolution of Pollution Levels from COVID-19 Lockdown to Post-Lockdown over India

Bhishma Tyagi ^{1,*} , Naresh Krishna Vissa ¹  and Sachin D. Ghude ²

¹ Department of Earth and Atmospheric Sciences, National Institute of Technology Rourkela, Rourkela 769008, India

² Indian Institute of Tropical Meteorology Pune, Pune 411008, India

* Correspondence: tyagib@nitrkl.ac.in

Abstract: The spread of the COVID-19 pandemic forced the administration to lock down in many countries globally to stop the spread. As the lockdown phase had only the emergency use of transportation and most of the industries were shut down, there was an apparent reduction in pollution. With the end of the lockdown period, pollution is returning to its regular emission in most places. Though the background was abnormally low in emissions (during the lockdown phase) and the reduced pollution changed the radiation balance in the northern hemispheric summer period, a modified pollution pattern is possible during the unlock phases of 2020. The present study analysed the unlock 1 and 2 stages (June–July) of the COVID-19 lockdown over India. The rainfall, surface temperature and cloud cover anomalies of 2020 for understanding the differences in pollutants variation were also analysed. The unlock phases show remarkable differences in trends and mean variations of pollutants over the Indian region compared to climatological variations. The results indicated changing high-emission regions over India to climatological variations and identified an AOD dipole with future emissions over India.

Keywords: COVID-19; unlock; emissions hotspots; AOD; air quality



Citation: Tyagi, B.; Vissa, N.K.; Ghude, S.D. Evolution of Pollution Levels from COVID-19 Lockdown to Post-Lockdown over India. *Toxics* **2022**, *10*, 653. <https://doi.org/10.3390/toxics10110653>

Academic Editors: Yoon-Hyeong Choi and Min Jae Ju

Received: 5 September 2022

Accepted: 27 October 2022

Published: 29 October 2022

Publisher's Note: MDPI stays neutral with regard to jurisdictional claims in published maps and institutional affiliations.



Copyright: © 2022 by the authors. Licensee MDPI, Basel, Switzerland. This article is an open access article distributed under the terms and conditions of the Creative Commons Attribution (CC BY) license (<https://creativecommons.org/licenses/by/4.0/>).

1. Introduction

The year 2020 had an exceptional COVID-19 spread, a pandemic claiming 806,543 deaths and 23,309,597 infections globally as of 23 August 2020 [1]. The pandemic has forced Governments in different parts of the world to lock down, which meant restricting movements, limited transportation, and the shutdown of industries and schools to prevent COVID-19 spread [2,3]. In addition to concerning health and economic issues during the lockdown [4–6], the COVID-19 lockdown resulted in a positive aspect of reducing pollution and reviving the environment globally [7,8]. Every major city around the globe witnessed a drastic reduction in pollutant concentrations during the pandemic spread period due to lockdown/restricted emission scenarios [9–11]. However, the magnitude of pollutant reduction varies spatially.

Various published manuscripts highlight the significant reductions in pollution during the COVID-19 lockdown globally. Although this work could not summarise all the findings, we summarised the findings by citing a few results from the published works to obtain a clear idea about air quality variations. Many works reported a significant reduction in various pollutants. Rodríguez-Urrego et al. [12] analysed Particulate matter with 2.5 micrometre or smaller diameter (PM_{2.5}) reductions over fifty most polluted capital cities of the world, including countries from Asia, Europe, and American continents, during COVID-19 lockdown and found an overall averaged 12% decrease in PM_{2.5} concentrations over these cities. Collivignarelli et al. [13] reported a reduction of ~32–40% in PM₁₀ (Particulate matter with 10 micrometre or smaller diameter) values, ~37–44% in PM_{2.5}, ~49% in benzene, ~57.6% in CO, ~20% in SO₂, ~47–51.4% in NO₂ over the city of Milan, Italy. Otmani et al. [14] showed that PM₁₀, SO₂ and NO₂ were reduced by 75%, 49% and 96%

during the COVID-19 lockdown over Salé City (Morocco). Tobias et al. [15] reported that the black carbon and NO₂ were reduced by 45 and 51%, while PM₁₀ was reduced by 28 to 31% in Barcelona (Spain) during the COVID-19 lockdown. They also found that O₃ levels increased from 33 to 57% for the eight hourly daily maxima during this period. Kerimray et al. [16] found that during the lockdown, the PM_{2.5}, CO and NO₂ concentrations were reduced by 21%, 49% and 35%, respectively, and O₃ levels increased by 15% during the lockdown over Almaty, Kazakhstan. The enhanced O₃ values due to reduced NO_x values were also reported by Sicard et al. [17]. They highlighted that Southern European cities (Nice, Rome, Valencia and Turin) have a different magnitude of variations in pollutants than Wuhan (China) during the lockdown, e.g., O₃ increase (17% in Europe, 36% in Wuhan) and PM reduced ~42% in Wuhan and ~8% in Europe, with a substantial reduction (~56%) in NO_x in all cities. Zalakeviciute et al. [18] reported reduced concentrations of NO₂ (−68%), SO₂ (−48%), CO (−38%) and PM_{2.5} (−29%) in the capital city of Quito, Ecuador, during COVID-19 lockdown period. Broomandi et al. [19] found a decrease in SO₂ by 5–28%, NO₂ by 1–33%, CO by 5–41% and PM₁₀ by 1.4–30%, respectively, over Tehran, Iran, during the COVID-19 lockdown period.

Pollution reduction is higher in major cities of developing countries such as India and China during the COVID-19 lockdown. Filonchik et al. [20] found that CO and NO₂ were reduced by 20% and 30%, while aerosol optical depth (AOD) and SO₂ were significantly reduced over East China during the COVID-19 Lockdown period. Bao and Zhang [21] analysed PM_{2.5}, PM₁₀, SO₂, NO₂ and CO over 44 cities in northern China and found a significant decrease in levels of all pollutants during the COVID-19 lockdown. India's megacities and state capitals reported a substantial pollution reduction during the COVID-19 lockdown period, e.g., [22,23]. Mahato et al. [24] found that PM_{2.5} and PM₁₀ were reduced by >50%, NO₂ by 52.68% and CO by 30.35% in Delhi, the capital of India, during the COVID-19 lockdown period. However, there are also reports of unperturbed air quality over specific zones over India during the COVID-19 lockdowns [25] related to power plant emissions. The main reason attributed to the reduced emissions of pollutants during the COVID-19 lockdown was the strict restriction on the movement of vehicles and the limited opening of industries [26]. The information is crucial and important to researchers, policy makers and the general public due to providing an unprecedented situation where in reality, one can measure the background pollution levels of different pollutants in different parts of the country [27,28].

Most global studies also reported a significant reduction in pollution during the COVID-19 lockdown period. Interestingly, a few studies report no decrease or increase in aerosol concentrations during the COVID-19 lockdown period. Nadzir et al. [29] found that PM_{2.5} and PM₁₀ increased to 60% and 9.7% during the lockdown period over Kota Damansara, an urban area of Klang Valley, Malaysia, while at other sites, there are reductions by ~20 to 60%. The fossil fuel burnings in the residential area of Kota Damansara are the reason for the increased PM levels. Similar observations of elevated/maintained aerosol concentrations were reported by Ranjan et al. [30] over the central and eastern Indian region, where coal mines were in continuous operation during the lockdown period. Hari et al. [31] reported increased atmospheric methane over India during the COVID-19 lockdown. Apart from the pollution concentration changes during the COVID-19 lockdown, studies reported the changes in GNSS signals [32], crop-residual burning patterns [33] and the link of pollution patterns to COVID-19 spread [34] in India.

The Government of India limits the lockdown period to 31 May 2020 and states unlock phase on 1 June 2020 with limited movement and unlock two on 1 July 2020 with more flexibility to move (<https://www.mygov.in/covid-19>) (accessed on 15 August 2020). As unlock phases start, the transportation and industrial sectors regrow their emissions back to their routine, and pollution growth increases to higher levels in a couple of months. Even during the unlock phases, the public is taking precautions and avoiding unnecessary travel in India, keeping pollution growth under control. Though there has been vast reporting of pollution drop during the COVID-19 lockdown, published works did not

extensively discuss the regrowth of pollution during the unlock phases in India. The present work analysed the pollution pattern change during the unlock phase 1 and 2 over India, compared the growth with the lockdown period of 2020 and understood the months of unlock/lockdown period of 2020 with climatological variation differences (2000–2019) for AOD, NO₂ and SO₂. We also analysed surface temperature, cloud cover, and rainfall anomalies for 2020 from the climatological means to understand the changes in the lockdown and unlock phases.

2. Materials and Methods

The area of study for the present work was India. The data on Aerosol Optical Depth (AOD) at 550 nm as a proxy for the aerosol load (PM pollution) were taken from the daily 1 × 1 degree resolution gridded level 3 collection 6.1 Dark Target Deep Blue (DT-DB) aerosol product of the Moderate Resolution Imaging Spectroradiometer (MODIS) on the Terra satellite [35] with an overpass at about 10:30 am local time. The product combines retrievals using the dark target algorithm [36,37] over water and the deep blue [38] algorithm over land and provides improved data coverage over both dark and bright surfaces [39,40]. The NO₂ and SO₂ daily data were obtained from the Ozone Monitoring Instrument (OMI) for April–July 2005 to 2020. For NO₂, we used OMNO2d, cloud-screened total and tropospheric column Level-3 daily global gridded dataset with a spatial resolution of 0.25 × 0.25 degrees [41,42]. The SO₂ datasets were analysed by OMSO2e data, which gives a total column density of SO₂ in the planetary boundary layer. It is a Level-3 daily global gridded dataset with a spatial resolution of 0.25 × 0.25 degrees [43]. For rainfall, daily precipitation data from 2000 to 2020 were adopted from Global Precipitation Mission (GPM) Integrated Multi-satellite Retrievals (IMERG) version V06, which has a resolution of 0.1-degree × 0.1-degree. We also employed ERA-5 reanalysis data fields of surface temperature and cloud cover information (monthly data) for India from 2000 to 2020. ERA-5 is the fifth generation of European reanalysis datasets produced by the European Centre for Medium-Range Weather Forecast (ECMWF) [44]. In order to calculate mean variations, we averaged the data for any parameter over the study area. The industrial and power plant locations with annual coal consumption and emissions related to coal-fired power plants are adopted from Guttikunda and Jawahar [45].

In the present work, we attempted to identify the differences in pollutants during the lockdown and unlock phases of 2020. In order to observe the difference pattern without the COVID-19 lockdown scenario, we used the same months' climatological variations. The work, therefore, is not commenting in any way that the COVID-19 lockdown or unlock phases changed the climatological patterns, but we are trying to understand the changes in 2020 with the help of climatological patterns.

3. Results

3.1. Understanding the Difference between Monsoon and Pre-Monsoon Variation

As the unprecedented COVID-19 lockdown allows studying baseline emissions, it is interesting to learn how the unlock period changed the pollution pattern after reduced pollution levels over India. We computed the difference between monsoon months (June–July) and pre-monsoon months (April–May) for the climatological period, i.e., 2000–2019 for AOD and 2005–2019 for NO₂ and SO₂ (Figure 1a–c). The difference between unlock phase (June–July 2020) and lockdown phase (April–May 2020) for AOD, NO₂, and SO₂ was computed (Figure 1d–f) to see how the change in pollution growth of these pollutants concerns long-term average values over India.

The long-term average difference between monsoon and pre-monsoon months shows negative values in AOD (Figure 1a) over south-eastern coastal regions and positive values over the north, central and western areas of India. The positive values were higher as we moved northward side of India, as the rainfall is less during June–July over those regions, and the rainout/washout of AOD is the least. The variation in NO₂ (Figure 1b) marks a decrease over India, including the Indo-Gangetic plains, except over a region

encompassing the northern states of Haryana, Punjab, Himachal Pradesh, and parts of Gujrat and Rajasthan, where the values are either slightly positive or zero. The SO₂ differences show positive values over the Indo-Gangetic plains, northern and western regions of India, and negative values over the rest of the Indian region (central, eastern, and southern parts). The results advocate that half of the country has higher values of SO₂ during monsoon, and the other half has lower emissions during monsoon months compared to pre-monsoon months. The positive/negative values over the upper/lower part of the country are directly related to rainfall patterns from June to July [46].

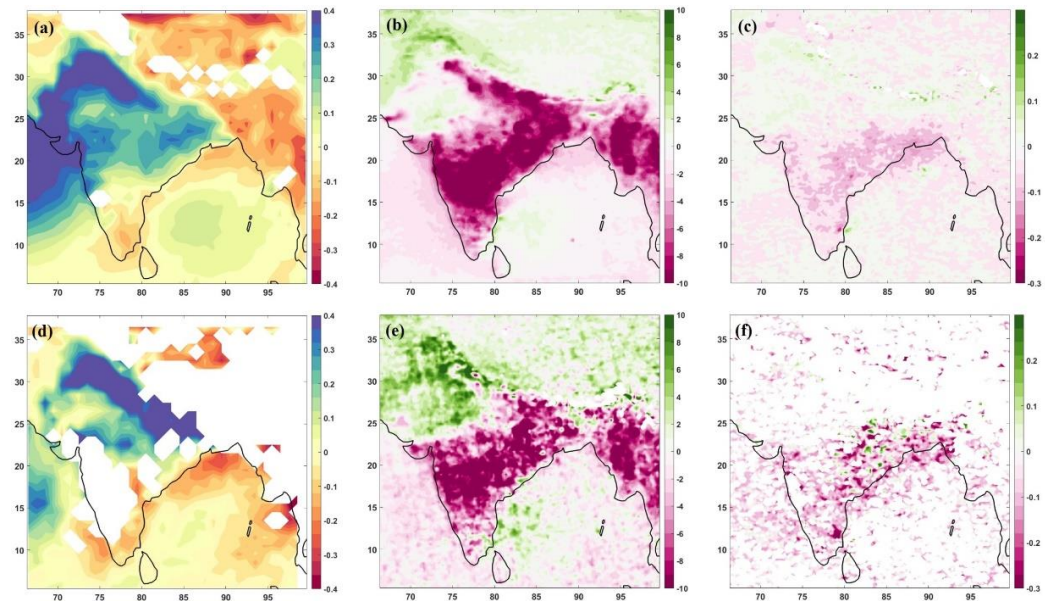


Figure 1. Difference between June–July and April–May values climatologically (upper row) and for 2020 (bottom row): AOD, left column: (a,d); NO₂, middle column: (b,e); SO₂, right column: (c,f). The AOD is dimensionless, NO₂ is ($\times 10^{15}$ molecules/cm²) and SO₂ is in Dobson Units [DU].

The difference in pollutants from unlock to lockdown phase of 2020 has a different variation compared to the climatological mean in AOD, NO₂ and SO₂. The AOD differences (Figure 1d) cannot provide complete information over the whole of India due to data gaps. However, it is clear from the analysis that the high positive values of AOD, which were up to north India (Haryana, Punjab and western Uttar Pradesh), are now extended to the complete Indo-Gangetic plain during 2020. The results indicate that during the unlock phase, the AOD values were higher over the Indo-Gangetic plain, which was expected as the lockdown phase reduced pollution levels. The eastern and coastal regions of India have differences similar to climatological values, indicating that rainfall controls the variation from June to July. Similar to AOD, the NO₂ variations (Figure 1e) also show higher values over the north and northwest sectors and lower values over the rest of India as climatological variations (Figure 1b). The higher values of NO₂ over the north and the northwest region show a clear impact of lockdown reduced NO₂ emissions in those regions due to reduced vehicular emissions, limited industrial activities, and controlled fossil fuel burning in household usage [44].

Interestingly, the rest of the country could not show such a marked difference from the unlock–lockdown period. The reasons may be continuous power plant operations and coal mining operations during the lockdown period (Ranjan et al., 2020). If we analyse SO₂ variation during 2020 (Figure 1f), the higher values over the Indo-Gangetic plain no longer exist. The reduced values over the rest of the Indian region are continuing, but there are regions with higher values over eastern India (Odisha, West Bengal and Jharkhand). The variational changes in SO₂ are reporting a reduction in SO₂ emissions even during the unlock phase of 2020 over the Indo-Gangetic plain and higher emissions at places marked

with industries and power-plants locations in eastern India. Though the results are not entirely unexpected, we needed to analyse the rainfall anomaly for the year 2020 for a better understanding of the differences discussed in the next section.

3.2. Rainfall Anomaly for the Year 2020

Figure 2 represents the rainfall anomaly for lockdown and unlock months of 2020 from the climatological mean of 2000–2019. For April (Figure 2a), the rainfall increased for the Indo-Gangetic plain and coastal belt from south to east, especially over the eastern Indian region (Odisha and West Bengal). Though there is no decrease in rainfall all over India, central India did not show any significant change in rainfall amount for April. May 2020 also marked higher rainfall (Figure 2b) over the Indian region. This month, the passage of supercyclone Amphan marked higher rainfall in the affected areas. The monsoon onset month of June (Figure 2c) had a different rainfall pattern in 2020 compared to April and May. The southwest coastal regions of India (Kerala and Karnataka) had deficit rainfall, while other southern states (Tamilnadu, Andhra Pradesh and Telangana) did not significantly change rainfall for the month. Higher precipitation was observed for the western part (Maharashtra and Gujrat), central India (Chhattisgarh, Madhya Pradesh and Rajasthan), eastern India (Odisha, West Bengal and Jharkhand) and parts of Indo Gangetic Plain (Uttar Pradesh and Bihar). The values were higher than April and May variations. For July 2020 (Figure 2d), the Indo Gangetic plain region (parts of Uttar Pradesh and Bihar) and northern and central India (Haryana, Punjab and Rajasthan) received higher rainfall amounts. Central India (Madhya Pradesh, Chhattisgarh) and the west coast of India (including regions of Maharashtra, Karnataka and Kerala) showed a significant decrease in rainfall for July 2020. When we combine the difference between monsoon and pre-monsoon months, there is a reduction in rainfall amount over the southwest coast of India and an increase in rainfall over the Indo-Gangetic plains.

3.3. AOD, NO₂ and SO₂ Anomalies for Lockdown and Unlock Phases of the Year 2020

Figure 3 shows the anomaly of the year 2020 from the climatology for the lockdown (April–May) and unlock phase (June–July) over the Indian region. The climatology was made only for April–May and June–July months (separately) to analyse these variations with respect to lockdown and unlock phases. One expects reduced pollutants in the lockdown phase and increased values during the unlock phases. However, the results are not as expected for unlock stages. The AOD values in the lockdown phase (Figure 3a) show a significant reduction over north-west regions (Haryana, Punjab, Himachal Pradesh, Delhi, Jammu and Kashmir, and parts of Uttar Pradesh). However, the eastern states of Odisha, West Bengal and Jharkhand show an increase in the values for the lockdown period. For the monsoon season, we had more missing data in AOD. Figure 3d indicates a higher decrease in the regions of the lockdown phase in addition to central and western Indian areas (Madhya Pradesh, Chhattisgarh, Gujrat and Maharashtra), where the increase over Odisha, West Bengal and Jharkhand was higher than that of lockdown phase, observed in Figure 3a.

The NO₂ variations over India during the lockdown phase (Figure 3b) show a decrease over the Indo-Gangetic plains and southern states of Tamilnadu, Andhra Pradesh and Telangana. At the same time, some hotspot regions were observable over eastern India (Odisha, West Bengal, and Jharkhand). When we checked the monsoon months (unlock phases), there was a uniform decrease in NO₂ of ~10 µg/m³ per day over India (Figure 3e). No hotspot was visible for the unlock phase in the NO₂ anomaly variations. As in the unlock phases, the movement started, and with usual traffic and industries, the NO₂ concentrations were supposed to return to typical values in 2020; this result was unexpected. The low concentrations indicate that the emissions were restricted even in the unlock phases. India uniformly shows reduced emissions, which was not even the case during the lockdown period. The uniform decrease during the unlock phases may also be attributed to higher

rainfall received during 2020 (Figure 2c,d), adding the rainout and washout of NO₂ in higher amounts.

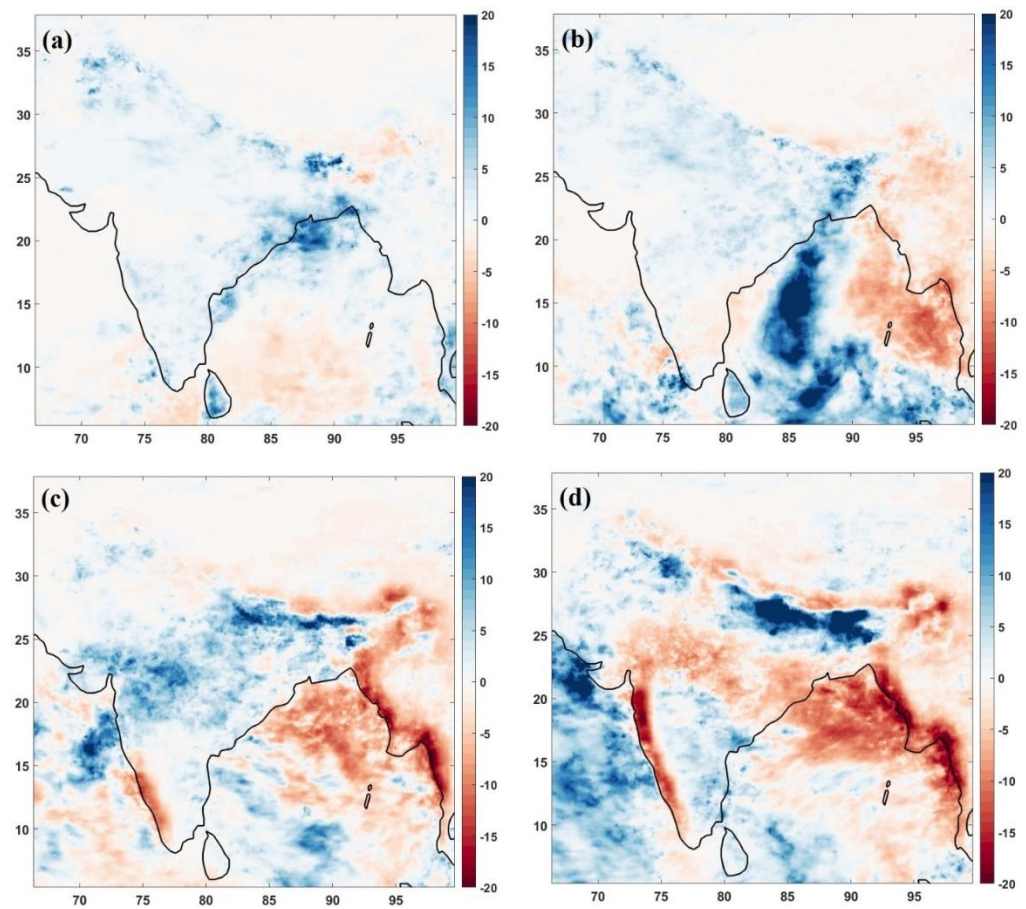


Figure 2. GPCC derived monthly rainfall anomaly of 2020 (from climatological mean of 2000–2019) for (a) April, (b) May, (c) June and (d) July. The units of rainfall are mm/month.

The SO₂ variations, though, are trivial to understand for the lockdown and unlock phases of 2020, as they can be connected to coal burning [47,48]. Unlike AOD or NO₂ variations, SO₂ anomalies during lockdown months (Figure 3c) show higher emissions at locations of coal-fired power plants in eastern regions (West Bengal, Odisha, and Jharkhand), south (Chennai) and a few places in north India. Other than these identified locations, the SO₂ concentrations showed a reduction over the whole of India. For the unlock months (Figure 3f), the eastern India region emerged as a higher emission region. West Bengal, Odisha and Jharkhand are the states with hotspot regions for SO₂ emission. The combined discharge from the mineral industries, mines and coal-fired power plants keeps the higher emissions of SO₂ over the area compared to the rest of the country. Even with higher rainfall (Figure 2) and a lockdown/unlock situation in place, the year 2020 marked higher SO₂ emissions over the eastern region from climatology, indicating the rise in production and capacity of various industrial establishments over the area [45].

3.4. Relationships between Meteorological and Air Quality Factors

The air pollutants variation during the COVID-19 lockdown and unlock phases were also impacted by the meteorological conditions during this period. Most of the studies explored the change in pollutants/emissions during the lockdown well, but the exploration of meteorological changes and their feedback process is less explored during these phases. The relationship between meteorological conditions and pollution changes was explored globally and found to have a feedback process between the two [49]. For the COVID-19 lockdown period, Singh et al. [26] explored the surface temperature, wind speed and

rainfall along with pollutants. They found that the existence of anticyclonic motion over the Bay of Bengal and the Arabian Sea, along with prevailing north westerlies, is one prominent feature observed during the lockdown years of 2020. The study reported that all the meteorological parameters follow a similar spatial variation, which was also confirmed by other studies, e.g., [22,50–52]. The reduced pollutant concentration also acted as a feedback process of impacting the meteorological parameters, and Pal et al. [53] reported a significant reduction in regional temperature related to emissions over India during the COVID-19 period. Moreover, the boundary layer height was ~70% higher, with a 40–60% increase in relative humidity and 20–40% slower wind speeds (on a synoptic scale) during the COVID-19 lockdown [54]; further making the available concentrations of pollutants to appear low.

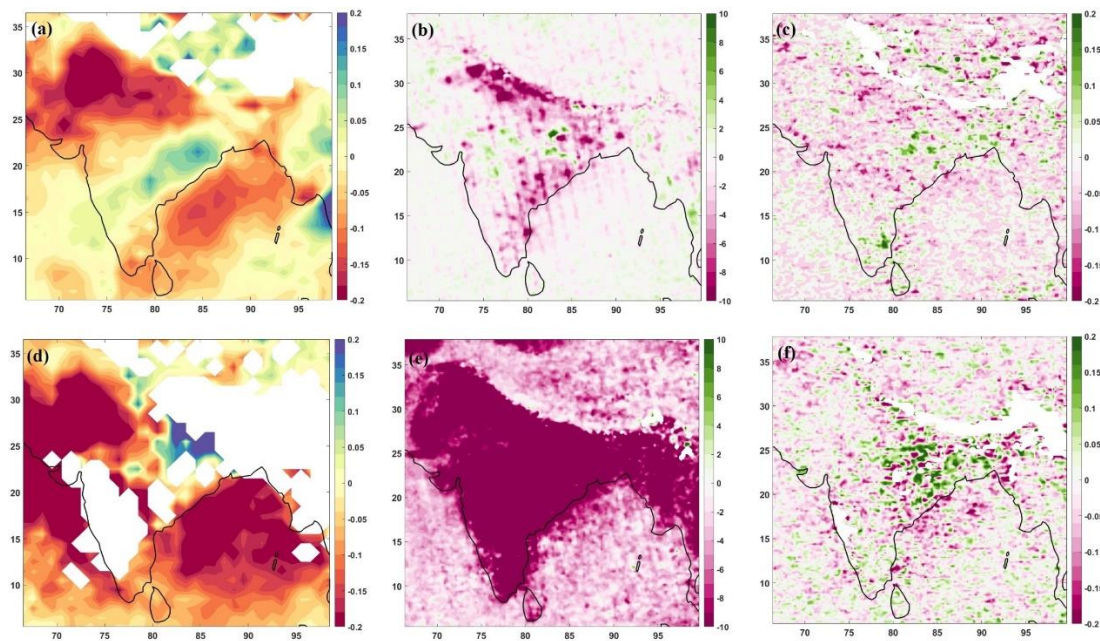


Figure 3. Anomaly of April–May (top row) and June–July (bottom row) from 2020 observations: AOD, left column: (a,d); NO₂, middle column: (b,e); SO₂, right column: (c,f). The AOD is dimensionless, NO₂ is ($\times 10^{15}$ molecules/cm²) and SO₂ is in Dobson Units [DU].

In order to further explore the relationship between the meteorological factors and pollutant concentrations, we analysed the surface temperature and cloud cover variations over the Indian region. The variations in surface temperature and cloud cover were explored for the same period as the pollutants for April–May and June–July. We utilised ERA5 reanalysis data to analyse the surface temperature and cloud cover over the Indian region, and Figure 4 depicts the anomalies of 2020 from the 2000–2019 values.

The lockdown phase temperature anomaly (Figure 4a) shows that a large part of India (including north India, Indo-Gangetic plains, and eastern India) has a negative temperature anomaly during the lockdown phase. However, the western and southern regions had positive anomaly values during the lockdown phase. During the lockdown phase, the cloud cover significantly increased over India, and the northern and eastern parts (including the Indo-Gangetic plains) showed up to a 15% increase in the cloud cover (Figure 4b). However, the central, western, and southern parts did not show any such increase in cloud cover during the lockdown; instead, there was a slight decrease in cloud cover values.

The temperature still shows a negative anomaly for the unlock phases over most of India. However, the magnitudes for a more prominent part are reduced, except over Bihar. The higher positive magnitude of anomaly over western India also shows a shift northward, i.e., over the adjoining Pakistan region in the unlock phase (Figure 4c). The cloud cover anomaly also has negative values over the northern part for unlock phases (Figure 4d).

However, the state of Bihar in north India still shows a positive anomaly. This creates a dipole pattern in the cloud cover over north India, where both positive and negative cloud cover anomalies are observed. The surface temperature and cloud cover anomalies show an inverse relationship (Figure 4). The pre-monsoon negative temperature anomalies are over the regions of positive cloud cover anomalies during the lockdown period (Figure 4a,b). Similarly, the negative temperature anomalies during the unlock phase agree with positive cloud cover anomalies during the unlock phase (Figure 4c,d).

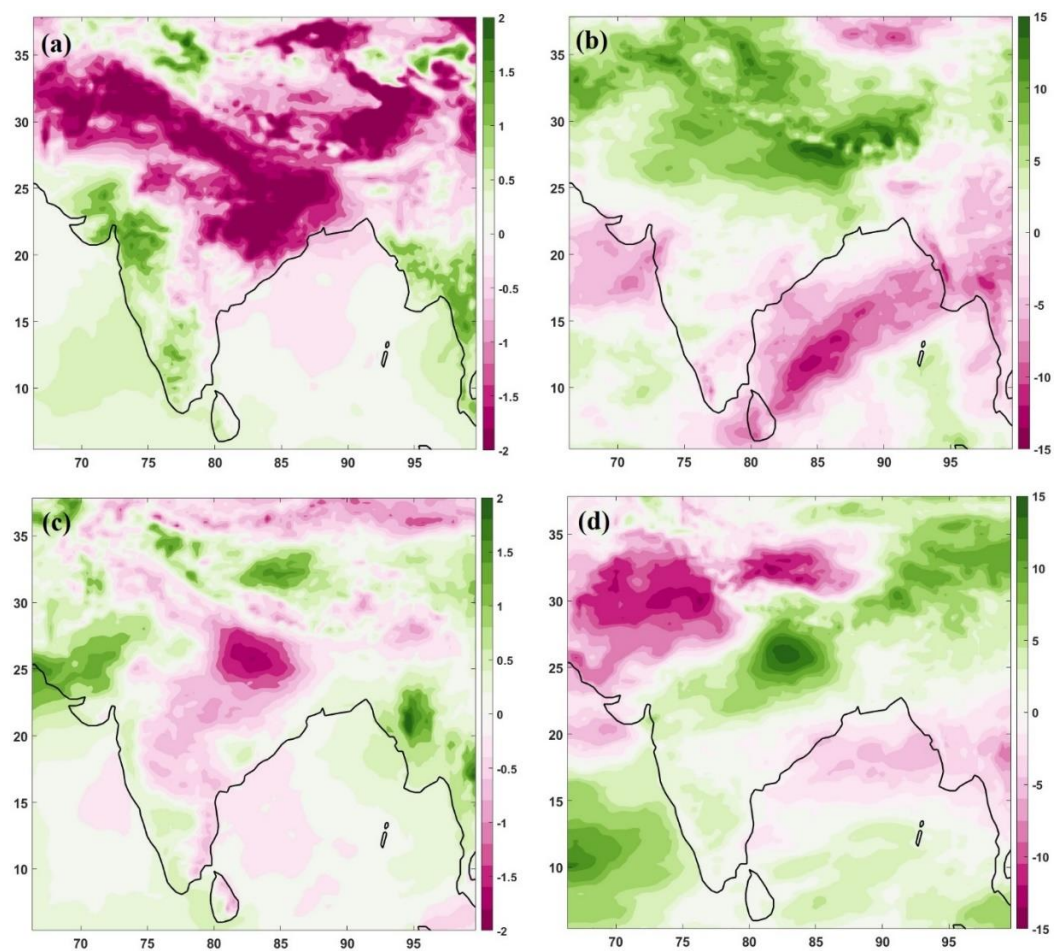


Figure 4. Anomaly of April–May (top row) and June–July (bottom row) from 2020 observations: surface temperature, left column: (a,c); cloud cover, right column: (b,d). Temperature is in K, and cloud cover is in percentage (%).

4. Discussion

The present study investigated the patterns of AOD, NO₂ and SO₂ during the lockdown and unlock phases of COVID-19 over India. The study incorporated the rainfall, surface temperature and cloud cover patterns for the same periods to understand better how the feedback between these meteorological variables and pollution evolved during the study period. The unique way of pollutant variation during the COVID-19 lockdown reduced pollution on average for the global scenario. The changes from lockdown to unlock phases differ from the previous emission patterns, where the pollution concentrations were relatively higher.

For the unlock phase, the pollution concentrations were not as high as they used to be in the climatology (Figure 1). However, the Indo-Gangetic plain emerged as the region of reduced aerosol pollution during the lockdown phase. When we analysed the variation in NO₂ and SO₂, the difference between unlock and lockdown phase indicated that the levels in unlock phases are showing reduced concentrations compared to the

lockdown phase over India, except in parts of northern and central India, which mark the impact of lockdown over NO_2 and SO_2 , with substantial reductions in concentrations. The precipitation anomalies (Figure 2) during the lockdown period show positive values over India. In contrast, during the unlock phases, the values are primarily positive over India in June. July offered a negative anomaly over central and southwest India, but there were increased (positive) anomalies over the Indo-Gangetic plain.

The unlock and lockdown phase anomalies from climatology (Figure 3) indicated that though most of India observed reduced pollution concentrations during the lockdown phase, the hotspots are visible over eastern India. However, more interestingly, the unlock phases show reduced pollution from climatological values for AOD and NO_2 for India. For SO_2 , the country shares a positive–negative anomaly map, indicating that the values increased/decreased over places for the country during the 2020 unlock period from the climatological values. The AOD dipole pattern over the Indian region [50] is evident in both pre-monsoon (lockdown) and monsoon (unlock) sub-sections.

We analysed India's surface temperature and cloud cover values (Figure 4) to find if the temperature and cloud cover feedback works with the pollutant variations over the country and attempt to identify the feedback mechanism. The surface temperature anomalies for unlock and lockdown phase from 2020 show a reduced temperature over the north, east and central India, with higher magnitudes during the lockdown period. The higher temperature regions were also observed over western India during the lockdown and unlock phases. Cloud cover showed an inverse relation to surface temperature, and the northern and eastern areas showed an increase in cloud cover during the lockdown phase. However, during the unlock phase, there was a significant reduction in cloud cover over the northern region. However, the eastern part continued to have higher cloud cover, which created a dipole structure in cloud cover. The temperature anomalies show a good agreement with AOD during the lockdown and unlock phases. The reduction/increase in temperature is related to the reduction/increase in AOD over northern, western and southern regions of India. However, the increased AOD over eastern India is not in agreement with reduced temperature during the lockdown. The temperature pattern changes are also in agreement with NO_2 variations during the lockdown phase, but the unlock phase is unable to explain the temperature dipole pattern over India. SO_2 concentrations are poorly correlated with temperature variations over India and not matching either with lockdown or unlock phases. During the unlock phase, India showed a negative anomaly in NO_2 during 2020 from the climatological values, with negative temperature and positive cloud cover anomaly values. One can also argue that as the lockdown was unprecedented and the reductions were primarily due to the absence of emission sources, one may not obtain the feedback mechanism between the temperature and cloud cover with the pollutants, which is the case in the present analysis. However, there may be feedback from pollution to meteorology, and the reduced temperature pattern during the unlock and lockdown phase can reduce the country's AOD, NO_2 and SO_2 values.

5. Conclusions

The lockdown and unlock phases related to COVID-19 in 2020 gave us a unique opportunity to understand the base levels of AOD, NO_2 and SO_2 and their sector-wise growth in India. The results show changed emission patterns during the COVID-19 times and significantly lower values during monsoon months (unlock phases 1 and 2) compared to climatological variations. We summarised the findings of the present work as follows:

- The difference between monsoon and pre-monsoon months climatology revealed that the north region has higher AOD values. During the COVID-19 unlock/lockdown phases, the extent of the higher AOD region extended to the total Indo-Gangetic plain. The AOD dipole existed during the anomaly of the lockdown and unlock stages of 2020. However, NO_2 variations were lower for the whole of India during unlock months and not for the lockdown period. The increased rainfall amounts in 2020 may

- be the reason. The SO₂ variations show hotspot emission regions over eastern India during both the lockdown and unlock phases compared to climatological variations;
- The NO₂ reduction during monsoon months to pre-monsoon months was evident in the whole of India except north region (Haryana, Punjab, Delhi, Himachal Pradesh, Rajasthan, Uttarakhand and parts of Uttar Pradesh) for climatological variations. However, during the COVID-19 times of 2020, the unlock months show a positive change (increase in values) over these states, which is different from the climatological variation. The SO₂ variations, however, move in line with climatological variations during 2020, except for higher emission SO₂ sites identified during the unlock–lockdown phase over Odisha, West Bengal and Jharkhand;
 - The COVID-19 lockdown and unlock months received higher rainfall than climatological variations over India. The surface temperature anomalies show reduced temperature for lockdown and unlock phases, more prominently during the lockdown. During the lockdown phase, there was an increase in cloud cover over northern and eastern India. In contrast, the unlock phases show a dipole pattern—a decrease over the northwestern part and an increase over east India.

The results indicated that during the unlock phase 1 (June–July 2020), the variations in AOD, NO₂ and SO₂ were smaller than climatological values due to reduced emissions associated with rainout and washout effects. There is a need to conduct a more comprehensive analysis to understand the reasons for such variations over different regions of India, particularly with surface temperature, radiation, and cloud cover during the study period.

Author Contributions: Conceptualization, B.T. and N.K.V.; methodology, B.T. and N.K.V.; software, B.T. and N.K.V.; formal analysis, B.T., N.K.V. and S.D.G.; investigation, B.T., N.K.V. and S.D.G.; resources, B.T., N.K.V. and S.D.G.; data curation, B.T. and N.K.V.; writing—original draft preparation, B.T. and N.K.V.; writing—review and editing, B.T., N.K.V. and S.D.G.; visualization, B.T. and N.K.V.; supervision, S.D.G. All authors have read and agreed to the published version of the manuscript.

Funding: This research received no external funding.

Data Availability Statement: Satellite data analysed for the study are freely accessible from <https://earthdata.nasa.gov/> (accessed on 1 March 2022). ERA5 datasets used in the study were obtained from <https://cds.climate.copernicus.eu/cdsapp#!/dataset/reanalysis-era5-land?tab=form> (accessed on 24 July 2022).

Acknowledgments: The authors are thankful to NASA Goddard Space Flight Center (GSFC) and Atmosphere Archive and Distribution System (LAADS) for making the level-3 MODIS datasets available. The authors are grateful to NASA, the OMI team and ECMWF for providing the NO₂, SO₂ and surface temperature and cloud cover datasets. The authors acknowledge the constant efforts of all the public and non-public institutions in tackling the global COVID-19 pandemic.

Conflicts of Interest: The authors declare no conflict of interest.

References

1. World Health Organization. Rolling Updates on Coronavirus Disease (COVID-19). 2020. Available online: <https://www.who.int/emergencies/diseases/novel-coronavirus-2019/events-as-they-happen> (accessed on 24 August 2020).
2. Koh, D. COVID-19 lockdowns throughout the world. *Occup. Med.* **2020**, *70*, 322. [CrossRef]
3. Lancet, T. India under COVID-19 lockdown. *Lancet* **2020**, *395*, 1315. [CrossRef]
4. Coibion, O.; Gorodnichenko, Y.; Weber, M. The Cost of the COVID-19 Crisis: Lockdowns, Macroeconomic Expectations, and Consumer Spending (No. W27141) (No. w27141). *Natl. Bur. Econ. Res.* **2020**, 27141. Available online: https://www.nber.org/system/files/working_papers/w27141/w27141.pdf (accessed on 15 August 2020).
5. Sibley, C.G.; Greaves, L.M.; Satherley, N.; Wilson, M.S.; Overall, N.C.; Lee, C.H.; Milojev, P.; Bulbulia, J.; Osborne, D.; Milfont, T.L.; et al. Effects of the COVID-19 pandemic and nationwide lockdown on trust, attitudes toward government, and well-being. *Am. Psychol.* **2020**, *75*, 618–630. [CrossRef] [PubMed]
6. Webb, L. COVID-19 lockdown: A perfect storm for older people’s mental health. *J. Psychiatr. Ment. Health Nurs.* **2020**, *28*, 300. [CrossRef] [PubMed]
7. Paital, B. Nurture to nature via COVID-19, a self-regenerating environmental strategy of environment in global context. *Sci. Total Environ.* **2020**, *729*, 139088. [CrossRef]

8. Barcelo, D. An environmental and health perspective for COVID-19 outbreak: Meteorology and air quality influence, sewage epidemiology indicator, hospitals disinfection, drug therapies and recommendations. *J. Environ. Chem. Eng.* **2020**, *8*, 104006. [[CrossRef](#)]
9. Zambrano-Monserrate, M.A.; Ruano, M.A.; Sanchez-Alcalde, L. Indirect effects of COVID-19 on the environment. *Sci. Total Environ.* **2020**, *728*, 138813. [[CrossRef](#)]
10. Muhammad, S.; Long, X.; Salman, M. COVID-19 pandemic and environmental pollution: A blessing in disguise? *Sci. Total Environ.* **2020**, *728*, 138820. [[CrossRef](#)]
11. Sahu, S.K.; Tyagi, B.; Beig, G.; Mangaraj, P.; Pradhan, C.; Khuntia, S.; Singh, V. Significant change in air quality parameters during the year 2020 over 1st smart city of India: Bhubaneswar. *SN Appl. Sci.* **2020**, *2*, 1990. [[CrossRef](#)]
12. Rodríguez-Urrego, D.; Rodríguez-Urrego, L. Air quality during the COVID-19: PM_{2.5} analysis in the 50 most polluted capital cities in the world. *Environ. Pollut.* **2020**, *266*, 115042. [[CrossRef](#)]
13. Collivignarelli, M.C.; Abbà, A.; Bertanza, G.; Pedrazzani, R.; Ricciardi, P.; Miino, M.C. Lockdown for COVID-2019 in Milan: What are the effects on air quality? *Sci. Total Environ.* **2020**, *732*, 139280. [[CrossRef](#)] [[PubMed](#)]
14. Otmami, A.; Benchrif, A.; Tahri, M.; Bounakhla, M.; El Bouch, M.; Krombi, M.H. Impact of COVID-19 lockdown on PM₁₀, SO₂ and NO₂ concentrations in Salé City (Morocco). *Sci. Total Environ.* **2020**, *735*, 139541. [[CrossRef](#)] [[PubMed](#)]
15. Tobías, A.; Carnerero, C.; Reche, C.; Massagué, J.; Via, M.; Minguillón, M.C.; Alastuey, A.; Querol, X. Changes in air quality during the lockdown in Barcelona (Spain) one month into the SARS-CoV-2 epidemic. *Sci. Total Environ.* **2020**, *726*, 138540. [[CrossRef](#)] [[PubMed](#)]
16. Kerimray, A.; Baimatova, N.; Ibragimova, O.P.; Bukenov, B.; Kenessov, B.; Plotitsyn, P.; Karaca, F. Assessing air quality changes in large cities during COVID-19 lockdowns: The impacts of traffic-free urban conditions in Almaty, Kazakhstan. *Sci. Total Environ.* **2020**, *730*, 139179. [[CrossRef](#)] [[PubMed](#)]
17. Sicard, P.; De Marco, A.; Agathokleous, E.; Feng, Z.; Xu, X.; Paoletti, E.; Rodriguez, J.J.D.; Calatayud, V. Amplified ozone pollution in cities during the COVID-19 lockdown. *Sci. Total Environ.* **2020**, *735*, 139542. [[CrossRef](#)]
18. Zalakeviciute, R.; Vasquez, R.; Bayas, D.; Buenano, A.; Mejia, D.; Zegarra, R.; Diaz, A.; Lamb, B. Drastic Improvements in Air Quality in Ecuador during the COVID-19 Outbreak. *Aerosol Air Qual. Res.* **2020**, *20*, 1530–1540. [[CrossRef](#)]
19. Broomandi, P.; Karaca, F.; Nikfal, A.; Jahanbakhshi, A.; Tamjidi, M.; Kim, J.R. Impact of COVID-19 Event on the Air Quality in Iran. *Aerosol Air Qual. Res.* **2020**, *20*, 0205. [[CrossRef](#)]
20. Filonchik, M.; Hurynovich, V.; Yan, H.; Gusev, A.; Shpilevskaya, N. Impact Assessment of COVID-19 on Variations of SO₂, NO₂, CO and AOD over East China. *Aerosol Air Qual. Res.* **2020**, *20*, 0226. [[CrossRef](#)]
21. Bao, R.; Zhang, A. Does lockdown reduce air pollution? Evidence from 44 cities in northern China. *Sci. Total Environ.* **2020**, *731*, 139052. [[CrossRef](#)]
22. Navinya, C.; Patidar, G.; Phuleria, H.C. Examining Effects of the COVID-19 National Lockdown on Ambient Air Quality across Urban India. *Aerosol Air Qual. Res.* **2020**, *20*, 0256. [[CrossRef](#)]
23. Singh, J.; Tyagi, B. Transformation of air quality over a coastal tropical station Chennai during covid-19 lockdown in India. *Aerosol Air Qual. Res.* **2020**, *21*, 200490. [[CrossRef](#)]
24. Mahato, S.; Pal, S.; Ghosh, K.G. Effect of lockdown amid COVID-19 pandemic on air quality of the megacity Delhi, India. *Sci. Total Environ.* **2020**, *730*, 139086. [[CrossRef](#)]
25. Tyagi, B.; Choudhury, G.; Vissa, N.K.; Singh, J.; Tesche, M. Changing air pollution scenario during COVID-19: Redefining the hotspot regions over India. *Environ. Pollut.* **2021**, *271*, 116354. [[CrossRef](#)] [[PubMed](#)]
26. Singh, V.; Singh, S.; Biswal, A.; Kesarkar, A.P.; Mor, S.; Ravindra, K. Diurnal and temporal changes in air pollution during COVID-19 strict lockdown over different regions of India. *Environ. Pollut.* **2020**, *266*, 115368. [[CrossRef](#)]
27. Ravindra, K.; Singh, T.; Biswal, A.; Singh, V.; Mor, S. Impact of COVID-19 lockdown on ambient air quality in megacities of India and implication for air pollution control strategies. *Environ. Sci. Pollut. Res.* **2021**, *28*, 21621–21632. [[CrossRef](#)] [[PubMed](#)]
28. Tibrewal, K.; Venkataraman, C. COVID-19 lockdown closures of emissions sources in India: Lessons for air quality and climate policy. *J. Environ. Manag.* **2022**, *302*, 114079. [[CrossRef](#)]
29. Nadzir, M.S.M.; Ooi, M.C.G.; Alhasa, K.M.; Bakar, M.A.A.; Mohtar, A.A.A.; Nor, M.F.F.M.; Latif, M.T.; Abd Hamid, H.H.; Ali, S.H.M.; Ariff, N.M.; et al. The Impact of Movement Control Order (MCO) during Pandemic COVID-19 on Local Air Quality in an Urban Area of Klang Valley, Malaysia. *Aerosol Air Qual. Res.* **2020**, *20*, 1237–1248. [[CrossRef](#)]
30. Ranjan, A.K.; Patra, A.K.; Gorai, A.K. Effect of lockdown due to SARS COVID-19 on aerosol optical depth (AOD) over urban and mining regions in India. *Sci. Total Environ.* **2020**, *745*, 141024. [[CrossRef](#)]
31. Hari, M.; Sahu, R.K.; Sunder, M.S.; Tyagi, B. Then and Now: COVID-19 Pandemic Lockdown Misfire Atmospheric Methane over India. *Aerosol Air Qual. Res.* **2022**, *22*, 210354. [[CrossRef](#)]
32. Kundu, B.; Panda, D.; Vissa, N.K.; Tyagi, B. Novel 2019 Coronavirus Outbreak" through the Eyes of GNSS Signal. *J. Geol. Soc. India* **2022**, *98*, 83–87. [[CrossRef](#)]
33. Hari, M.; Sahu, R.K.; Tyagi, B.; Kaushik, R. Reviewing the crop residual burning and aerosol variations during the COVID-19 pandemic hit year 2020 over North India. *Pollutants* **2021**, *1*, 127–140. [[CrossRef](#)]
34. Sahu, S.K.; Mangaraj, P.; Beig, G.; Tyagi, B.; Tickle, S.; Vinoj, V. Establishing a link between fine particulate matter (PM_{2.5}) zones and COVID-19 over India based on anthropogenic emission sources and air quality data. *Urban Clim.* **2021**, *38*, 100883. [[CrossRef](#)] [[PubMed](#)]

35. Platnick, S.; Hubanks, P.; Meyer, K.; King, M.D. MODIS Atmosphere L3 Monthly Product (08_L3). *NASA MODIS Adapt. Process. Syst. Goddard Space Flight Cent.* **2015**. Available online: https://doi.org/10.5067/MODIS/MOD08_M3.006 (accessed on 15 August 2020).
36. Levy, R.C.; Remer, L.A.; Mattoo, S.; Vermote, E.F.; Kaufman, Y.J. Second-generation operational algorithm: Retrieval of aerosol properties over land from inversion of Moderate Resolution Imaging Spectroradiometer spectral reflectance. *J. Geophys. Res. Atmos.* **2007**, *112*, 7811. [[CrossRef](#)]
37. Levy, R.C.; Mattoo, S.; Munchak, L.A.; Remer, L.A.; Sayer, A.M.; Patadia, F.; Hsu, N.C. The Collection 6 MODIS aerosol products over land and ocean. *Atmos. Meas. Tech.* **2013**, *6*, 2989–3034. [[CrossRef](#)]
38. Hsu, N.C.; Jeong, M.J.; Bettenhausen, C.; Sayer, A.M.; Hansell, R.; Seftor, C.S.; Huang, J.; Tsay, S.C. Enhanced Deep Blue aerosol retrieval algorithm: The second generation. *J. Geophys. Res. Atmos.* **2013**, *118*, 9296–9315. [[CrossRef](#)]
39. Bilal, M.; Qiu, Z.; Campbell, J.R.; Spak, S.N.; Shen, X.; Nazeer, M. A new MODIS C6 Dark Target and Deep Blue merged aerosol product on a 3 km spatial grid. *Remote Sens.* **2018**, *10*, 463. [[CrossRef](#)]
40. Wei, J.; Peng, Y.; Guo, J.; Sun, L. Performance of MODIS Collection 6.1 Level 3 aerosol products in spatial-temporal variations over land. *Atmos. Environ.* **2019**, *206*, 30–44. [[CrossRef](#)]
41. Krotkov, N.A.; Lamsal, L.N.; Celarier, E.A.; Swartz, W.H.; Marchenko, S.V.; Bucsela, E.J.; Chan, K.L.; Wenig, M.; Zara, M. The version 3 OMI NO₂ standard product. *Atmos. Meas. Tech.* **2017**, *9*, 3133–3149. [[CrossRef](#)]
42. Krotkov, N.A.; Lamsal, L.N.; Marchenko, S.V.; Celarier, E.A.; Bucsela, E.J.; Swartz, W.H.; Joiner, J.; the OMI core team. *OMI/Aura NO₂ Cloud-Screened Total and Tropospheric Column L3 Global Gridded 0.25 Degree × 0.25 Degree V3*; NASA Goddard Space Flight Center, Goddard Earth Sciences Data and Information Services Center (GES DISC): Greenbelt, MD, USA, 2019. Available online: https://disc.gsfc.nasa.gov/datasets/OMNO2d_003/summary (accessed on 15 August 2020).
43. Krotkov, N.A.; Li, C.; Leonard, P. *OMI/Aura Sulfur Dioxide (SO₂) Total Column L3 1 day Best Pixel in 0.25 Degree × 0.25 Degree V3*; Goddard Earth Sciences Data and Information Services Center (GES DISC): Greenbelt, MD, USA, 2015. Available online: https://disc.gsfc.nasa.gov/datasets/OMSO2e_003/summary (accessed on 15 August 2020).
44. Hersbach, H.; Bell, B.; Berrisford, P.; Horanyi, A.J.M.S.; Sabater, J.M.; Nicolas, J.; Radu, R.; Schepers, D.; Simmons, A.; Soci, C.; et al. Global reanalysis: Goodbye ERA-Interim, hello ERA5. *ECMWF Newsl.* **2019**, *159*, 17–24. [[CrossRef](#)]
45. Guttikunda, S.K.; Jawahar, P. Evaluation of particulate pollution and health impacts from planned expansion of coal-fired thermal power plants in India using WRF-CAMx modeling system. *Aerosol Air Qual. Res.* **2018**, *18*, 3187–3202. [[CrossRef](#)]
46. Guhathakurta, P.; Rajeevan, M. Trends in the rainfall pattern over India. *Int. J. Climatol.* **2008**, *28*, 1453–1469. [[CrossRef](#)]
47. Karplus, V.J.; Zhang, S.; Almond, D. Quantifying coal power plant responses to tighter SO₂ emissions standards in China. *Proc. Natl. Acad. Sci. USA* **2018**, *115*, 7004–7009. [[CrossRef](#)]
48. Guttikunda, S.K.; Jawahar, P. Atmospheric emissions and pollution from the coal-fired thermal power plants in India. *Atmos. Environ.* **2014**, *92*, 449–460. [[CrossRef](#)]
49. Cheng, N.; Zhang, D.; Li, Y.; Xie, X.; Chen, Z.; Meng, F.; Gao, B.; He, B. Spatiotemporal variations of PM_{2.5} concentrations and the evaluation of emission reduction measures during two red air pollution alerts in Beijing. *Sci. Rep.* **2017**, *7*, 8220. [[CrossRef](#)]
50. Vissa, N.K. and Tyagi, B. Aerosol dipole pattern over India: Consequences on rainfall and relation with wind circulations. *Acta Geophys.* **2021**, *69*, 2475–2482. [[CrossRef](#)]
51. Sharma, S.; Zhang, M.; Gao, J.; Zhang, H.; Kota, S.H. Effect of restricted emissions during COVID-19 on air quality in India. *Sci. Total Environ.* **2020**, *728*, 138878. [[CrossRef](#)] [[PubMed](#)]
52. Biswal, A.; Singh, V.; Singh, S.; Kesarkar, A.P.; Ravindra, K.; Sokhi, R.S.; Chipperfield, M.P.; Dhomse, S.S.; Pope, R.J.; Singh, T. and Mor, S. COVID-19 lockdown-induced changes in NO₂ levels across India observed by multi-satellite and surface observations. *Atmos. Chem. Phys.* **2021**, *21*, 5235–5251. [[CrossRef](#)]
53. Pal, S.C.; Chowdhuri, I.; Saha, A.; Chakraborty, R.; Roy, P.; Ghosh, M.; Shit, M. Improvement in ambient-air-quality reduced temperature during the COVID-19 lockdown period in India. *Environ. Develop. Sustain.* **2021**, *23*, 9581–9608. [[CrossRef](#)]
54. Madineni, V.R.; Dasari, H.P.; Karumuri, R.; Viswanadhapalli, Y.; Perumal, P.; Hoteit, I. Natural processes dominate the pollution levels during COVID-19 lockdown over India. *Sci. Rep.* **2021**, *11*, 15110. [[CrossRef](#)]